Piezoelectric wafer active sensors for sensing acoustic emission due to crack rubbing/clapping

Roshan Joseph, Md Yeasin Bhuiyan, Victor Giurgiutiu

Roshan Joseph, Md Yeasin Bhuiyan, Victor Giurgiutiu, "Piezoelectric wafer active sensors for sensing acoustic emission due to crack rubbing/clapping," Proc. SPIE 10967, Active and Passive Smart Structures and Integrated Systems XII, 109672A (21 March 2019); doi: 10.1117/12.2515314

SPIE.

Event: SPIE Smart Structures + Nondestructive Evaluation, 2019, Denver, Colorado, United States

Piezoelectric wafer active sensors for sensing acoustic emission due to crack rubbing/ clapping

Roshan Joseph, Md Yeasin Bhuiyan, Victor Giurgiutiu

Department of Mechanical Engineering, University of South Carolina, Columbia, USA

1 ABSTRACT

Crack rubbing or clapping in metallic structures generates acoustic emission (AE) signals. Such AE signals need to be distinguished from AE signal due to fatigue crack growth event. AE signal due to crack rubbing or clapping of fatigue generated crack was studied for a plate specimen. 20 mm fatigue crack was generated in a 1 mm thick aluminum plate specimen. Vibration-induced excitation was performed on the specimen to induce crack faying surface-motion for AE signal generation. Various specimen resonances have different crack faying surface motions, which were studied from FEM analysis. Modeshapes and crack faying surface motions of the specimen are studied at 35 Hz and 180 Hz specimen resonances. AE signals at various specimen resonances were recorded by piezoelectric wafer active sensors (PWAS) and the recorded waveforms are analyzed to obtain AE signatures. At various specimen resonances, AE signals have different signatures due to the change in crack faying surface motions. AE recording was done by using multiple PWAS sensors placed at various distances from the crack. The difference in AE signals close to crack and distant from crack as well as the geometric spreading of AE signals originating due to crack rubbing was studied from multi-sensor experiments.

2 INTRODUCTION

For mechanical components that are frequently subjected to variable loading, fatigue cracking is a common problem. There are several theories developed over the years on fatigue as well as static crack growth problem. Theoretical and experimental developments on crack growth rate, stress intensity factor, plastic zones during crack growth and strain as well as stress field measurements around the crack region during crack growth were well explored, and much research is happening nowadays on these topics. Acoustic emission technique was widely used for damage detection and source localization. The vibration of mechanical components can induce rubbing and clapping of crack faying surfaces and thus can potentially cause an acoustic emission source. This paper aims at the study of piezoelectric wafer active sensors for detection of vibration induced crack rubbing and clapping acoustic emission signals.

AE signals may be generated by a wide range of phenomena such as micro-cracks, friction in existing cracks, dislocations, phase transformations, etc. The AE wave field generated by an AE event propagates in thin-wall structures such as plates in the form of guided waves. Many researchers studied AE due to various kinds of sources. Acoustic emission in thin plates during crack growth event was investigated in many researches[1], [2]. Acoustic emission due to rubbing in a rotor-bearing and source localization was studied by Wang et al. [3]. Acoustic emission in composite materials was also studied for progressive damage in a polymer-based composite[4]; clustering of AE signals obtained from failure in carbon fiber reinforced plastic (CFRP) specimens was also studied[5]. Acoustic emission during various fracture activities was studied to relate the fracture and AE signals [6]. McBride et al [7] investigated the relationship between acoustic emission amplitude and size of intermetallic inclusions at the fracture face. Barile et al [8] used the acoustic emission technique to monitor delamination in a unidirectional CFRP subjected to

Active and Passive Smart Structures and Integrated Systems XII, edited by Alper Erturk, Proc. of SPIE
Vol. 10967, 109672A · © 2019 SPIE · CCC code: 0277-786X/19/$18 · doi: 10.1117/12.2515314

mode I loading. They concluded that it is possible to follow delamination effects in CFRP through proper monitoring of variation of the AE features. Various studies on acoustic energy harvesting was reported in the literatures[9]–[11].

Many researchers have done numerical and theoretical modeling and simulation of AE signals. Some of the studies performed numerical modeling of AE signals using Lamb waves[12], [13]. Finite element modeling and simulation of AE forward problem was performed [14]–[17]. Monopole or dipole definition of AE sources was used for modeling AE sources in several studies[18]. Definition of AE source by considering the AE source as a self-equilibrating seismic moment tensor was studied, and analytical formulations were developed for half-space and bulk medium in many pieces of research [19] [20]. In a recent study of AE guided wave propagation in a plate [21], the AE source was modeled as Helmholtz excitation potentials.

Even though AE due to various phenomena was reported, not many research works were conducted on AE due to rubbing and clapping of crack faying surfaces of thin sheet metals. It is a problem of practical interest since it is important to distinguish between AE due to crack rubbing and crack growth during fatigue crack growth event. This paper presents the detection of AE signals due to rubbing and clapping of thin metallic sheet metal samples

The organization of this paper is as follows. First, this paper discusses the experimental methods used for generation of AE signals due to rubbing and clapping of crack faying surfaces. In this section, the manufacturing of the cracked specimen and experimental set-up for inducing crack faying surface motion on the specimen through the vibration of the specimen is discussed. Then, finite element modal analysis of the cracked specimen undergoing vibration excitation is presented. The resonant frequencies of the specimen, modeshapes and crack faying surface motions of the crack in the specimen during resonances are discussed. Next, the results of AE signals due to vibration-induced crack rubbing and clapping of the fatigue cracked specimen was presented. Finally, this paper ends with summary, conclusions and future work.

3 EXPERIMENTAL METHODS

3.1 SPECIMEN PREPARATION AND EXPERIMENTAL SETUP

Aluminum 2024-T3 specimen was chosen for manufacturing the test specimen material. The material properties of the specimen were 73 GPa modulus of elasticity, 2767 kg/m^{3}density, and 0.33 poisons ratio. The aluminum specimen manufactured was 103 mm width and 305 mm length and 1 mm thickness in dimensions. 1 mm hole was drilled at the geometric center of the specimen for initiating fatigue crack. The hole would cause stress concentration at the edges of the hole, and the crack initiation would happen at the hole. Fatigue loading was applied on the specimen to generate the pre-crack. For the pre-crack generation fatigue loading from 22 kN to 2.2 kN at a frequency of 4 Hz was applied. Crack initiation started approximately 40,600 cycles. Crack grew 20 mm in 400 cycles. After generating the crack in the specimen, four PWAS sensors were bonded on the specimen. One PWAS was bonded very close to the crack at a distance of 6 mm from the crack. This PWAS has bonded such a close distance so that it can pick up even the weak AE signals originating from the crack. Two other PWAS were bonded at 25 mm distance from the crack in opposite directions, and another PWAS was bonded at 50 mm from the crack. The PWAS bonding configuration and the time of arrival and amplitude of the signals reaching these PWAS would confirm the AE signal source and geometric spreading of the AE signals.

Figure 1 Experimental set up for fatigue crack growth. Cyclic fatigue loading was applied on the specimen by mounting the specimen on MTS machine.

The experimental setup for generating crack rubbing and clapping in the specimen is presented in Figure 2. For AE generation due to crack rubbing, the fatigue crack grew plate specimen was mounted on a shaker. Continuous sinusoidal excitation was given to the specimen at various frequencies through the shaker. The vibration of the specimen causes the faying surfaces of the crack to rub/clap each other. This rubbing and clapping produce acoustic emission signals.

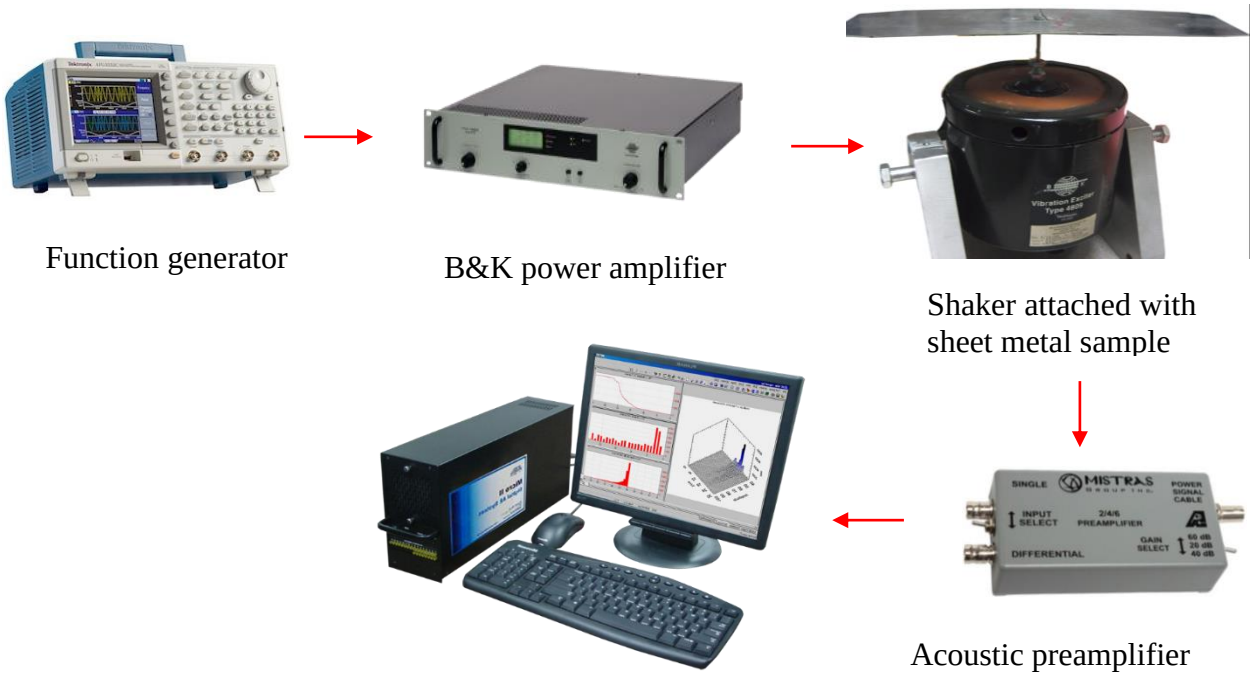

Figure 2 Experimental set up for capturing vibration AE signals

For the generation of continuous vibration, a function generator was used. For obtaining sufficient voltage of excitation, the signal is amplified using a power amplifier. The amplified sinusoidal signals are fed to a vibration exciter.

The shaker vibrates the plate in out of plane direction causing rubbing/clapping of crack faying surfaces and generation of AE signal due to the rubbing/clapping. The PWAS installed on the specimen sensed AE hits. Four identical preamplifiers with a built-in bandpass filter (30- 700 kHz) were connected to the sensors. The preamplifier is connected to Mistras AE system. A sampling frequency of 10 MHz was chosen to capture any high-frequency AE signals. AE hits at plate resonance were captured and analyzed. At plate resonances, the possibility of crack rubbing, as well as the threshold of AE signals, are higher, which makes it suitable for AE signal collection and analysis.

4 FEM ANALYSIS RESULTS

The relative motion of the crack-induced rubbing of the crack faying surfaces. At different frequencies, the crack faying surface motion depends on the mode shape of the specimen at that frequency. To understand the specimen resonances, mode shapes and crack faying surface motions, finite element (FE) analysis of specimen mounted on the shaker was performed. ANSYS software was used for the analysis.

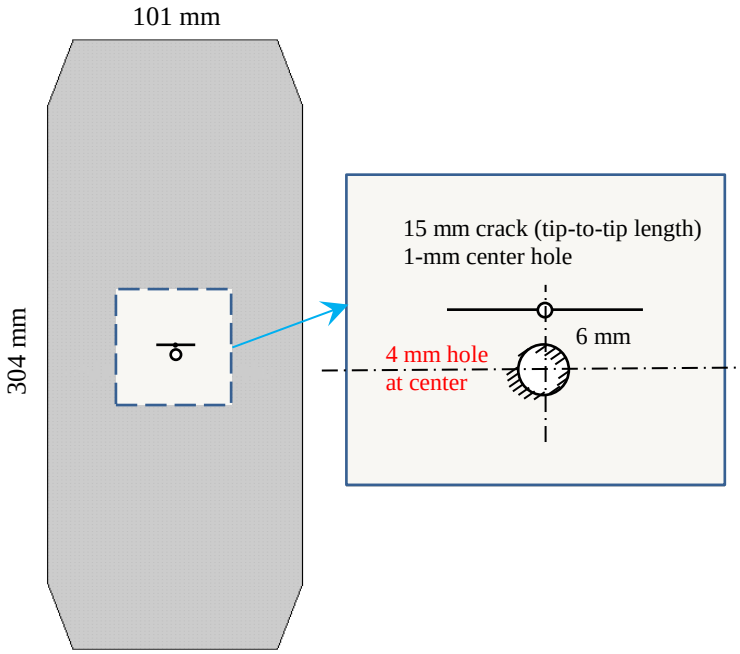

Figure 3 The specimen and boundary conditions given for performing modal analysis of specimen attached to shaker. Fixed boundary conditions are given at the support hole corresponding to the vibration shaker support.

The geometry of the cracked specimen was modeled using the ANSYS software. ANSYS mesh tool was used to mesh the geometry. Shell 63 element was chosen as the element type. Shell 63 element in ANSYS 17 has both bending and membrane capabilities. Both in-plane and normal loads are permitted. The element has six degrees of freedom at each node: translation in the nodal

x, y, and z directions and rotations about the nodal x, y, and z axes. For large deflection analyses, a consistent tangent stiffness matrix option is available. The material properties of the element were chosen as the material properties of aluminum 2024-T3 (73 GPa modulus of elasticity, 2767 kg/m^{3}density, and 0.33 poisons ratio). The specimen is fixed tightly to the shaker using bolted joint at the support hole. Hence the specimen support hole has a fixed boundary condition. For the FEM analysis, a fixed boundary condition was given at the support hole by arresting all 6 degrees of freedom of the nodes. The specimen modeled using ANSYS with the boundary conditions is shown in Figure 3.

Modal analysis of the specimen was performed by using the ANSYS 17 software. The result was post-processed to obtain resonance frequencies and corresponding mode shapes of the specimen. Each resonance frequency has different modeshape corresponding to it. The number of nodes and anti-nodes in the modeshapes increases at higher resonant frequencies. The position of nodes and anti-nodes also changes for different resonant frequencies. For high amplitude acoustic emission signal generation, the modeshape motion near the crack location is very important. If the modeshape motion near the crack location is favorable for an active crack faying surface motion, stronger AE signals would be generated.

The resonance frequencies of the priestine and the cracked specimen are presented in Table 1. For specimen with crack case the resonance frequency is slightly less than for specimen without the crack case. This change is due to the reduction in the stiffness of the specimen due to the presence of the crack.

Table 1 Resonances of the specimen attached to vibration applicator from FEM modal analysis. A slight change in resonance due to the presence of crack can be observed.

	Frequency (Hz)	
	No crack (Hz)	Crack at 6 mm (Hz)
1	30.3	28.2
2	38.1	37.8
3	95.6	93.1
4	112.3	112.3
5	193.5	188.4

Two different specimen frequencies were chosen for generating AE signals by inducing crack faying surface motions on the specimen, 35 Hz and 188 Hz. The modeshape of the specimen and crack faying surface motions at 35 Hz, and 188 Hz are presented in Figure 4. At 35 Hz the plate modeshape has a maximum displacement at the geometric center of the specimen and minimum displacements at ends of the specimen. Hence the modeshape have one node and two anti-nodes as we observe. The crack faying surface motion at 35 Hz is presented in Figure 4b. We observe there is a crack faying surface motion at the crack due to the modeshape deformation near the crack. The modeshape of the specimen at 180 Hz resonance is presented Figure 4c. At 180 Hz resonance, the specimen has a maximum displacement at the upper edge of the specimen and

minimum displacement at the lower edge of the specimen. Hence there are two nodes and two antinodes at this frequency of vibration of the specimen. The specimen has more nodes and antinodes compared to vibration at 35 Hz. The crack faying surface motion at 180 Hz resonance is also presented in Figure 4d. We observe a different topology of the crack faying surface motion at 180 Hz vibration of the specimen compared to 35 Hz vibration.

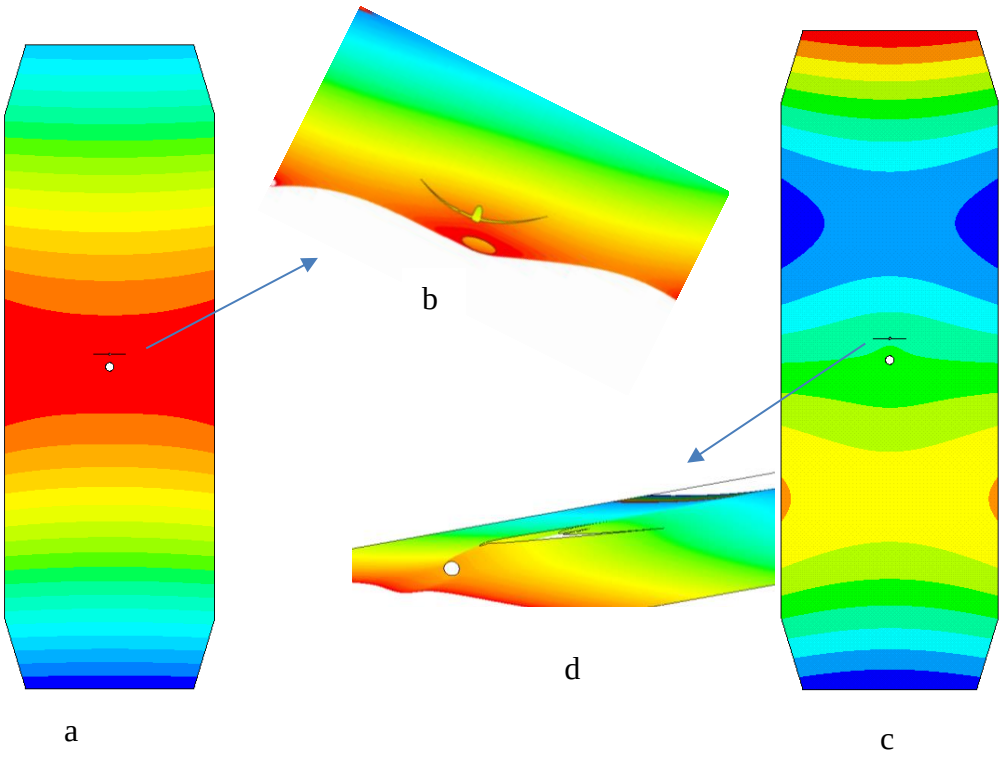

Figure 4 Mode shapes and crack faying surface motions of specimen under investigation at various resonance frequencies of specimen attached to shaker a) Modeshape of specimen at 35 Hz resonance b) Crack faying surface motion at 35 Hz resonance c) Modeshape of specimen at 188 Hz resonance b) Crack faying surface motion at 188 Hz resonance

5 EXPERIMENTAL RESULTS AND DISCUSSION

5.1.1 AE source localization

A confirmation of AE signals were originating from the crack is performed by AE source localization using multiple PWAS sensors. The time of arrival at various PWAS, as well as the amplitude of the AE signals, were analyzed for the confirmation. Four PWAS receivers were installed on the specimen numbered PWAS 1, PWAS 2, PWAS 3 and PWAS 4 respectively. PWAS 2 is the closest to the crack, at a distance of 5 mm. PWAS 1 and PWAS 3 are at a distance of 25 mm from the crack. PWAS 4 is located at a distance of 50 mm from the crack. The specimen was vibrated at a frequency 35 Hz for the source localization analysis. A particular AE event originating from the crack and reaching various PWAS receivers was identified from the time of arrivals obtained from the AE system and is presented in Table 2. Since PWAS 2 is the closest to the crack, the highest amplitude of 41 mV was observed at PWAS 2 among amplitudes at all

PWAS. Due to geometric spreading signal reaching PWAS 3, which is at a distance 25 mm from the crack has only 12 mV amplitude. PWAS 1 and 3 are of similar distance from the crack, but signal reaching PWAS 1 is 8 mV amplitude, less than the signal amplitude at PWAS 3. The AE signals traveling from crack to PWAS 1 undergo scattering at the vibration exciter attached to the specimen. Because of the scattering of AE signals at the vibration exciter, a lower amplitude of AE signal was observed at PWAS 1 in comparison with PWAS 3 even though the sensors are at the same distance from the crack. The relative time of arrival and amplitudes of AE signals obtained from Mistras AE system is presented in Table 2. The observed relative amplitude of AE signals at various PWAS, time of arrival, and sequence of arrival are possible only if the origin of the AE signal is at the crack. This analysis confirms that the AE signals are originating from the crack.

Table 2 Time of arrival and sequence of arrival of AE signals at various PWAS. PWAS 1 is the closest to the crack; hence AE signals arrive first at PWAS 1. PWAS 2 and PWAS 3 are equidistant from the crack. Hence AE signals arrive approximately same time. This analysis confirms that AE signals are originating from the crack.

	Time of arrival (Relative)	Sequence of arrival
PWAS 1	82	3
PWAS 2	66	1
PWAS 3	78	2

5.1.2 AE signal signature at 35 Hz resonance

As we have discussed in section 0, the resonant frequencies of specimen vibration are appropriate for the generation of strong displacements of the specimens. This strong displacement causes strong crack faying surface motions which can generate strong AE signal. We observe strong AE signal generation at 35 Hz frequency of vibration of the specimen. Vibration excitation was given to the specimen at 35 Hz by using a shaker, and the vibration induces the crack faying surface rubbing and clapping. The induced rubbing and clapping of the crack faying surfaces cause the excitation and propagation of AE signals in the specimen. The signals collected and the correlation of AE signals was presented in Figure 5. The AE signal signature is observed to be wideband. Peaks in the frequency spectrum were observed at 100 kHz. At frequency spectrum between 300-400 kHz, a peak in the frequency spectrum by gradual increment and decrement was also observed. The differences in signals are due to the uncertainty in AE source characteristic at the crack faying surfaces corresponding to various events. The minor difference in AE signal infers that, even though there is uncertainty in AE source characteristic which generates the AE signals, the source characteristics are within a tolerance limit.

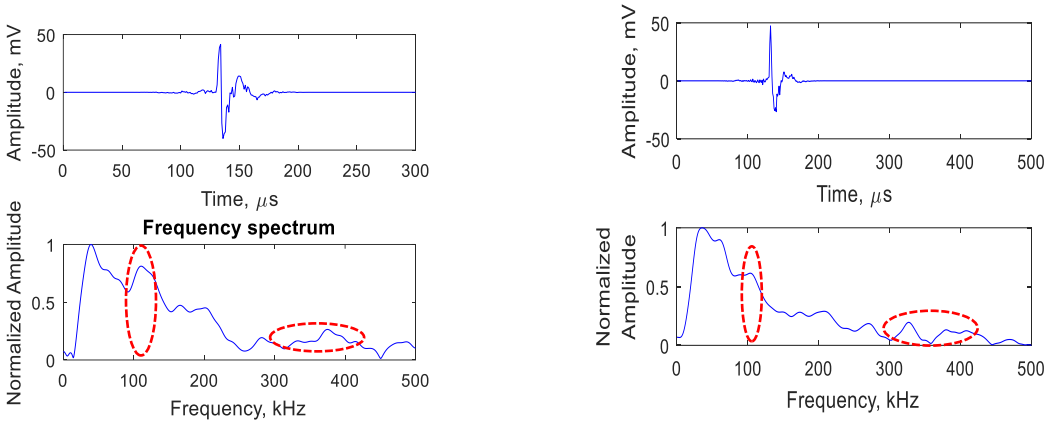

Figure 5 AE sample signals measured due to rubbing and clapping of crack faying surfaces of specimen at 35 Hz vibration a) sample signal 1 b) sample signal 2

5.1.3 AE signal signature at 180 Hz resonance

To study the effect of the frequency of vibration of the specimen on the AE signal, another frequency of vibration of the specimen was also considered. AE signals received by PWAS when the plate is vibrated at 180 Hz frequency is presented in Figure 6. We observe that the frequency spectrum of the AE signals is wideband frequency spectra. At 180 Hz vibration of the specimen also a peak frequency approximately at 100 kHz was observed, and a gradual increase and decrease of frequency spectrum between 300- 400 kHz was also observed. AE signals were observed to have a similar signature.

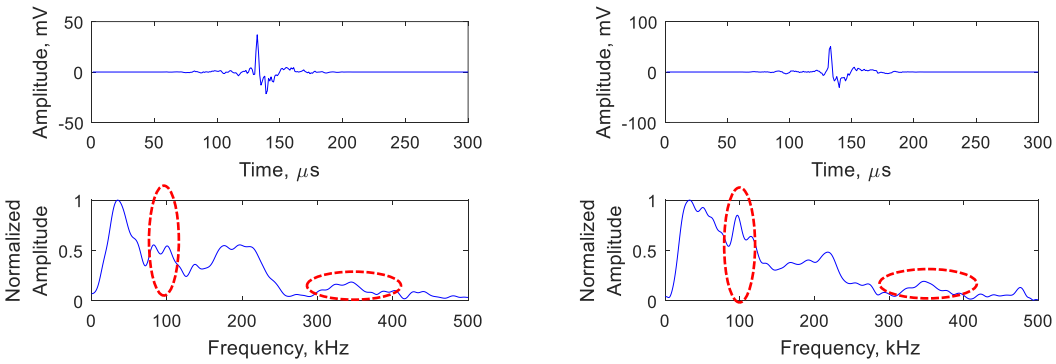

Figure 6 AE sample signals measured due to rubbing and clapping of crack faying surfaces of specimen at 180 Hz vibration a) sample signal 1 b) sample signal 2

The crack faying surfaces formed during the fatigue experiment is very rough in texture with sharp peaks and valleys. The vibration of the specimen causes the sharp peaks and valleys of crack faying surfaces to hit each other and generate AE signals. Hence the AE signal generation source can be

considered as a point force excitation source or a point source. AE signals are generated by rubbing of crack faying surfaces at a point. Even at different frequencies the source characteristic or the mechanism of ultrasonic AE signal generation may remain same since it is a point source excitation. Hence theoretically, it is very less likely that the AE signal signature may differ at different vibration exciter frequencies. A comparison of AE signal signature at 35 Hz vibration and 180 Hz vibration is presented in Figure 7. Clear similarities in AE signals and signal frequency spectrum is observed in the figure. The AE signal rise time, as well as the duration of the signal, is observed as approximately same. Frequency spectrums of both signals were found very similar with broadband nature and very similar peaks and valleys.

5.1.4 Comparison of signals

A comparison of typical AE signal recorded at 35 Hz specimen vibration and 180 Hz specimen vibration is presented in Figure 7. Both signals are very similar in the time domain as well as in the frequency domain. The rise time of the signal for both signals are approximately the same and the duration of the signals are also approximately 50 µs. Frequency spectra of both signals have a peak approximately at 100 kHz and a gradual increase and decrease in the frequency spectra between 300 kHz and 400 kHz. Even though the frequency of excitation is different, the overall signal characteristic is the same. AE signals are generated by rubbing of crack faying surfaces at a point. Even at different frequencies the source characteristic or the mechanism of ultrasonic AE signal generation may remain the same since it is a point source excitation. Hence theoretically, it is much less likely that the AE signal signature may differ at different vibration exciter frequencies. Minor changes in the frequency spectrum are observed because of the uncertainty in the source characteristic.

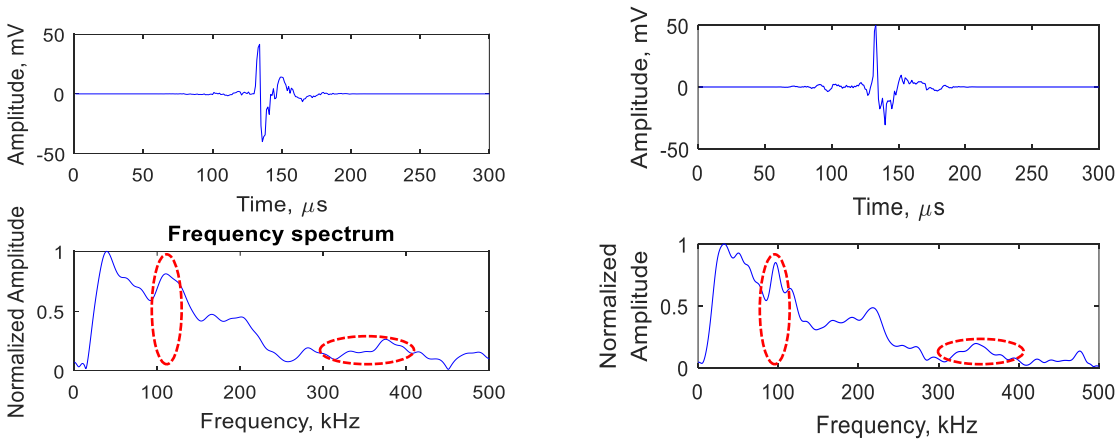

Figure 7 Comparison of AE signals at 35 Hz and 180 Hz vibration of the specimen. Signals at these frequencies were found similar a) Typical AE signal signature at 35 Hz b) Typical AE signal signature at 180 Hz

6 SUMMARY CONCLUSIONS AND FUTURE WORK

Fatigue crack in an Aluminum 2024-T3 specimen was generated by cyclic fatigue loading. Experimental set up for generating and recording AE signal due to rubbing and clapping of crack faying surfaces of the fatigue cracked specimen was designed. FEM modal analysis of specimen attached to the experimental set up was performed, and resonant frequencies, as well as modeshapes of the specimen, was studied. Crack faying surface motions at the resonant frequencies of the specimen was studied from FEM analysis. AE signals were generated and recorded through vibration induced crack faying surface motion in the specimen.

AE signals due to vibration of the specimen at 35 Hz and 180 Hz vibration of the specimen was studied. AE signal signatures at both the cases were found very similar. The AE signals generated by rubbing and clapping of crack faying surfaces were generated by hitting of peaks and valleys in the crack each other. This hitting is a point interaction with a very small area of contact. The excitation hence can be considered as a point source. The AE source characteristic in both cases would be the same.

This work can be extended to study about the AE signal due to crack rubbing and clapping of cracks of different lengths to study the influence of crack length on the AE signal signature.

7 ACKNOWLEDGEMENTS

This work was supported by the Air Force Office of Scientific Research (AFOSR) grant number FA9550-16-1-0401 and Office of Naval Research (ONR) grant number N00014-17-1-2829.

8 REFERENCES

[1] M. Y. Bhuiyan and V. Giurgiutiu, “The signatures of acoustic emission waveforms from fatigue crack advancing in thin metallic plates,” *Smart Mater. Struct.*, vol. 27, no. 1, p. 15019, 2018.

[2] H. Mei, M. Haider, R. Joseph, A. Migot, and V. Giurgiutiu, “Recent Advances in Piezoelectric Wafer Active Sensors for Structural Health Monitoring Applications,” *Sensors*, vol. 19, no. 2, p. 383, 2019.

[3] Q. Wang and F. Chu, “Experimental determination of the rubbing location by means of acoustic emission and wavelet transform,” *J. Sound Vib.*, vol. 248, no. 1, pp. 91–103, Nov. 2001.

[4] M. Bentahar and R. El Guerjouma, “Monitoring progressive damage in polymer-based composite using nonlinear dynamics and acoustic emission,” *J. Acoust. Soc. Am.*, vol. 125, no. 1, pp. EL39-EL44, 2009.

[5] M. G. R. Sause, A. Gribov, A. R. Unwin, and S. Horn, “Pattern recognition approach to identify natural clusters of acoustic emission signals,” *Pattern Recognit. Lett.*, vol. 33, no. 1, pp. 17–23, Jan. 2012.

[6] S. M. Cousland and C. M. Scala, “Acoustic emission during the plastic deformation of aluminium alloys 2024 and 2124,” *Mater. Sci. Eng.*, vol. 57, no. 1, pp. 23–29, Jan. 1983.

[7] S. L. McBride, J. W. MacLachlan, and B. P. Paradis, “Acoustic emission and inclusion fracture in 7075 aluminum alloys,” *J. Nondestruct. Eval.*, vol. 2, no. 1, pp. 35–41, 1981.

[8] C. Barile, C. Casavola, and G. Pappalettera, "Acoustic emission waveform analysis in CFRP under Mode I test," *Eng. Fract. Mech.*, no. December 2017, pp. 0–1, 2018.

[9] S. B. M. Saadatzi, F. Mir, M. N. Saadatzi, V. Tavaf, "Modeling of a 3D acoustoelastic metamaterial energy harvester," in *Active and Passive Smart Structures and Integrated Systems XII*, 2018.

[10] S. B. M. Saadatzi, F. Mir, M. N. Saadatzi, "Modeling and Fabrication of a Multi-axial Piezoelectric Energy Harvester based on a Metamaterial-inspired Structure," *IEEE Sens. J.*, vol. 18, no. 22, 2018.

[11] S. B. M. Saadatzi, M. N. Saadatzi, R. Ahmed, "An electro-dynamic 3-dimensional vibration test bed for engineering testing," in *Industrial and Commercial Applications of Smart Structures Technologies*, 2017.

[12] R. Joseph, M. Y. Bhuiyan, and V. Giurgiutiu, "Acoustic emission source modeling in a plate using buried moment tensors," *Proc. SPIE (Health Monit. Struct. Biol. Syst.*, vol. 10170, no. May, pp. 1017028-1–8, 2017.

[13] R. Joseph *et al.*, "Active health monitoring of TN32 dry cask using a scaled down model," *Proc. SPIE (Health Monit. Struct. Biol. Syst*, no. March, 2018.

[14] M. G. R. Sause and S. Horn, "Simulation of Acoustic Emission in Planar Carbon Fiber Reinforced Plastic Specimens," *J. Nondestruct. Eval.*, vol. 29, no. 2, pp. 123–142, 2010.

[15] M. Åberg, "Numerical modeling of acoustic emission in laminated tensile test specimens," *Int. J. Solids Struct.*, vol. 38, pp. 6643–6663, 2001.

[16] G. J. Prosser WH, Hamstad MA, "Finite Element and Plate Theory Modeling of Acoustic Emission Waveforms," *J Nondestruct Eval*, vol. 18, pp. 83–90, 1999.

[17] A. Zelenyak, M. Hamstad, and M. Sause, "Modeling of Acoustic Emission Signal Propagation in Waveguides," *Sensors*, vol. 15, no. 5, pp. 11805–11822, 2015.

[18] M. A. Hamstad, A. O'Gallagher, and J. Gary, "Modeling of buried monopole and dipole sources of acoustic emission with a finite element technique," *J. Acoust. Emiss.*, vol. 17, no. 3/4, pp. 97–110, 1999.

[19] J. R. Rice, "Elastic wave emission from damage process," *J. Nondestruct. Eval.*, vol. 1, no. 4, pp. 215–224, 1980.

[20] P. G. Keiiti A, *Quantitative Seismology*. University Science Books, 2002.

[21] Y. Haider, M. F., Giurgiutiu, V., Lin, B. and Yu, "Simulation of Lamb Wave Propagation using Excitation Potentials," in *ASME 2017 Pressure Vessels & Piping Conference*, 2017.